

## Visible Light Generation of Iodine Atoms and I–I Bonds: Sensitized I<sup>−</sup> Oxidation and I<sub>3</sub><sup>−</sup> Photodissociation

James M. Gardner, Maria Abrahamsson, Byron H. Farnum, and Gerald J. Meyer\*

*Departments of Chemistry and Materials Science & Engineering, Johns Hopkins University,  
3400 North Charles Street, Baltimore, Maryland, 21218*

Received June 18, 2009; E-mail: meyer@jhu.edu

**Abstract:** Direct 355 or 532 nm light excitation of TBAI<sub>3</sub>, where TBA is tetrabutyl ammonium, in CH<sub>3</sub>CN at room temperature yields an iodine atom, I<sup>•</sup>, and an iodine radical anion, I<sub>2</sub><sup>•−</sup>. In the presence of excess iodide, the iodine atom reacts quantitatively to yield a second equivalent of I<sub>2</sub><sup>•−</sup> with a rate constant of  $k = 2.5 \pm 0.4 \times 10^{10} \text{ M}^{-1} \text{ s}^{-1}$ . The I<sub>2</sub><sup>•−</sup> intermediates are unstable with respect to disproportionation and yield initial reactants,  $k = 3.3 \pm 0.1 \times 10^9 \text{ M}^{-1} \text{ s}^{-1}$ . The coordination compound Ru(bpz)<sub>2</sub>(deeb)(PF<sub>6</sub>)<sub>2</sub>, where bpz is 2,2'-bipyrazine and deeb is 4,4'-(C<sub>2</sub>H<sub>5</sub>CO<sub>2</sub>)<sub>2</sub>-2,2'-bipyridine, was prepared and characterized for mechanistic studies of iodide photo-oxidation in acetonitrile at room temperature. Ru(bpz)<sub>2</sub>(deeb)<sup>2+</sup> displayed a broad metal-to-ligand charge transfer (MLCT) absorption band at 450 nm with  $\epsilon = 1.7 \times 10^4 \text{ M}^{-1} \text{ cm}^{-1}$ . Visible light excitation resulted in photoluminescence with a corrected maximum at 620 nm, a quantum yield  $\phi = 0.14$ , and an excited state lifetime  $\tau = 1.75 \mu\text{s}$  from which  $k_r = 8.36 \times 10^4 \text{ s}^{-1}$  and  $k_{nr} = 5.01 \times 10^5 \text{ s}^{-1}$  were abstracted. Arrhenius analysis of the temperature dependent excited state lifetime revealed an activation energy of  $\sim 2500 \text{ cm}^{-1}$  and a pre-exponential factor of  $10^{10} \text{ s}^{-1}$ , assigned to activated surface crossing to a ligand field or MLCT excited state. Steady state light excitation of Ru(bpz)<sub>2</sub>(deeb)<sup>2+</sup> in a 20 mM TBAI acetonitrile solution resulted in ligand loss photochemistry with a quantum yield of  $5 \times 10^{-5}$ . The MLCT excited state was dynamically quenched by iodide with  $K_{sv} = 1.1 \times 10^5 \text{ M}^{-1}$  and  $k_q = 6.6 \pm 0.3 \times 10^{10} \text{ M}^{-1} \text{ s}^{-1}$ , a value consistent with diffusion-limited electron transfer. Excited state hole transfer to iodide was quantitative but the product yield was low due to poor cage escape yields,  $\phi_{CE} = 0.042 \pm 0.001$ . Nanosecond transient absorption was used to quantify the appearance of two photoproducts [Ru(bpz<sup>−</sup>)(bpz)(deeb)]<sup>+</sup> and I<sub>2</sub><sup>•−</sup>. The coincidence of the rate constants for [Ru(bpz<sup>−</sup>)(bpz)(deeb)]<sup>+</sup> formation and for excited state decay indicated reductive quenching by iodide. The rate constant for the appearance of I<sub>2</sub><sup>•−</sup> was about a factor of 3 slower than excited state decay,  $k = 2.4 \pm 0.2 \times 10^{10} \text{ M}^{-1} \text{ s}^{-1}$ , indicating that I<sub>2</sub><sup>•−</sup> was not a primary photoproduct of excited state electron transfer. A mechanism was proposed where an iodine atom was the primary photoproduct that subsequently reacted with iodide,  $\text{I}^{\bullet} + \text{I}^{-} \rightarrow \text{I}_2^{\bullet-}$ . Charge recombination  $\text{Ru}(\text{bpz}^{-})(\text{bpz})(\text{deeb})^{+} + \text{I}_2^{\bullet-} \rightarrow \text{Ru}(\text{bpz})_2(\text{deeb})^{2+} + 2\text{I}^{-}$  was highly favored,  $\Delta G^{\circ} = -1.64 \text{ eV}$ , and well described by a second-order equal concentration kinetic model,  $k_{cr} = 2.1 \pm 0.3 \times 10^{10} \text{ M}^{-1} \text{ s}^{-1}$ .

### Introduction

Oxidation of aqueous iodide solutions results in the high yield formation of I–I bonds.<sup>1</sup> The photo-oxidation of iodide is therefore of general interest to the growing community of scientists that hope to store energy from the sun in the form of chemical bonds.<sup>2</sup> Molecular details of light initiated electron transfer reactions that result in chemical bond formation are rare,<sup>3,4</sup> particularly with regard to photodissociative excited states where bonds are irreversibly broken.<sup>5</sup> Thus, there exists a fundamental need to identify assemblies of materials, compounds, and/or ions that enable integration of light absorption

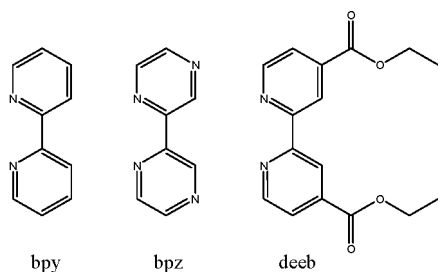
with chemical bond formation. Sensitized iodide oxidation provides such an opportunity and a molecular basis for the conversion of solar photons into chemical energy stored in I–I covalent bonds.<sup>6–11</sup> In principle, this chemical energy can be converted to electrical power in galvanic or fuel cells.

A promising coordination compound for excited state iodide oxidation reactions is Ru(bpz)<sub>2</sub>(deeb)<sup>2+</sup>, where bpz is 2,2'-bipyrazine and deeb is 4,4'-(C<sub>2</sub>H<sub>5</sub>CO<sub>2</sub>)<sub>2</sub>-2,2'-bipyridine, Scheme 1. The study of Ru(II) bipyrazine compounds was pioneered by Lever and co-workers who have clearly demonstrated the

- (1) Stanbury, D. M. *Adv. Inorg. Chem.* **1989**, *33*, 69.
- (2) Lewis, N. S.; Nocera, D. G. *Proc. Natl. Acad. Sci. U.S.A.* **2006**, *103*, 15729.
- (3) Heyduk, A. F.; Nocera, D. G. *Science* **2001**, *293*, 1639.
- (4) Esswein, A. J.; Veige, A. S.; Nocera, D. G. *J. Am. Chem. Soc.* **2005**, *127*, 16641.
- (5) Geoffroy, G. L.; Wrighton, M. S. *Organometallic Photochemistry*; Academic Press: New York, 1979.

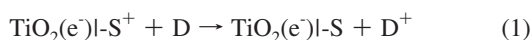
- (6) Crutchley, R. J.; Lever, A. B. P. *J. Am. Chem. Soc.* **1980**, *102*, 7128.
- (7) Clark, C. C.; Marton, A.; Meyer, G. J. *Inorg. Chem.* **2005**, *44*, 3383.
- (8) Marton, A.; Clark, C. C.; Srinivasan, R.; Freundlich, R. E.; Narducci-Sarjeant, A. A.; Meyer, G. J. *Inorg. Chem.* **2006**, *45*, 362.
- (9) Gardner, J. M.; Giaimuccio, J. M.; Meyer, G. J. *J. Am. Chem. Soc.* **2008**, *130*, 17252.
- (10) Maestri, M.; Bolletta, F.; Moggi, L.; Balzani, V.; Henry, M. S.; Hoffman, M. Z. *J. Chem. Soc., Chem. Commun.* **1977**, 491.
- (11) Sexton, D. A.; Curtis, J. C.; Cohen, H.; Ford, P. C. *Inorg. Chem.* **1984**, *23*, 49.

## Scheme 1



strong oxidizing power of their excited states.<sup>1,6,12–15</sup> Compounds like Ru(bpz)<sub>3</sub><sup>2+</sup>, are thermodynamically capable of excited state water oxidation while this same reaction is unfavored for Ru(bpy)<sub>3</sub><sup>2+</sup>.<sup>16</sup> For photogalvanic and dye sensitization studies, the ethyl ester groups of the deeb ligands can be hydrolyzed to carboxylic acids to yield 4,4'-(CO<sub>2</sub>H)<sub>2</sub>-2,2'-bipyridine, dcb, that bind strongly to wide band gap metal oxide semiconductors like TiO<sub>2</sub>.<sup>17,18</sup> For the fluid acetonitrile studies reported herein, Ru(bpz)<sub>2</sub>(deeb)(PF<sub>6</sub>)<sub>2</sub> is more soluble and straightforward to purify than the corresponding compound with a dcb ligand.

The oxidation of iodide to the complex anion tri-iodide, I<sub>3</sub><sup>-</sup>, in acetonitrile is of particular importance to the function of regenerative dye sensitized solar cells based on mesoporous nanocrystalline (anatase) TiO<sub>2</sub> thin films, that is, Grätzel cells.<sup>17,18</sup> Iodide quantitatively regenerates the sensitizer after excited state injection, and the resultant I<sub>3</sub><sup>-</sup> oxidation product does not efficiently recombine with electrons in the TiO<sub>2</sub> nanocrystallites, TiO<sub>2</sub>(e<sup>-</sup>). It is this latter property of I<sup>-</sup>/I<sub>3</sub><sup>-</sup> that makes it special. Several outer-sphere electron donors, D, have been identified that promote quantitative *regeneration* of the sensitizer, S, eq 1, but a relatively small fraction of the oxidized donors, D<sup>+</sup>, escape the mesoporous thin film before *recombination* with TiO<sub>2</sub>(e<sup>-</sup>), eq 2.<sup>19</sup>

**Regeneration:****Recombination:**

Remarkably, I<sub>3</sub><sup>-</sup> is reduced at the counter electrode of gold-standard dye sensitized solar cells nearly quantitatively such that absorbed photon-to-current efficiencies are within experimental uncertainty of unity at the short circuit condition. Perhaps even more impressive is the fact that the current decreases very little, <5%, at the power point where about 10 electrons are expected to reside in each TiO<sub>2</sub> nanocrystallite.<sup>18</sup> While the effect of recombination on the photocurrent is known to be negligible, reaction 2 is thought to have a significant influence on the quasi-Fermi level of the sensitized TiO<sub>2</sub> thin film and hence influences the photovoltage and overall power conversion efficiency.<sup>18,19</sup>

The extremely low efficiency of Reaction 2 when D<sup>+</sup> is I<sub>3</sub><sup>-</sup> has made experimental quantification difficult. However, studies with systematic variations in the molecular structure of the sensitizer, S, have provided some insights. Examples where charge recombination was *enhanced* through Lewis acid-base adduct formation between the sensitizer and I<sub>3</sub><sup>-</sup> (or I<sub>2</sub>) have been reported.<sup>20–22</sup> On the other hand, recombination has been *inhibited* with phenyl-ethyne spacers between the carboxylic acid anchoring groups and the redox active metal center.<sup>23</sup> There also exists some evidence that the important electron acceptor is not I<sub>3</sub><sup>-</sup> but rather iodine, I<sub>2</sub> or its reduced radical anion, I<sub>2</sub><sup>•-</sup>.<sup>24</sup> These species are present in such low concentrations in dye sensitized solar cells that it would rationalize the miniscule yield of unwanted charge recombination provided that some explanation existed for the lack of reactivity with I<sub>3</sub><sup>-</sup> that is typically present in 50 mM concentrations.

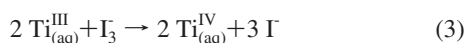
There are at least two appealing, possibly related, yet unproven explanations for sluggish reactions of TiO<sub>2</sub>(e<sup>-</sup>) with I<sub>3</sub><sup>-</sup>. The first is that charge recombination is unfavored due to the large reorganization energy associated with breaking I–I bonds. For dissociative electron transfer the bond energy is included in the total reorganization energy so a large internal contribution is expected for Reaction 2 when I<sub>3</sub><sup>-</sup> is the acceptor.<sup>25</sup> In support of this hypothesis, we note that the only alternative redox mediators that are at all useful in dye sensitized solar cells are based on Co<sup>III/II</sup> and Cu<sup>II/I</sup> diimine compounds whose self-exchange rate constants are unusually small due to large internal reorganization energy changes imparted by spin and coordination number changes, respectively.<sup>26,27</sup>

The second explanation is that the TiO<sub>2</sub>(e<sup>-</sup>)s are good one electron reductants, perhaps best thought of as Ti(III) trap states, that are unable to facilitate the 2e<sup>-</sup> reduction of I<sub>3</sub><sup>-</sup>, which is in fact the only reaction observed for I<sub>3</sub><sup>-</sup> at metallic electrodes.<sup>28–30</sup> In addition, quinone/hydroquinone redox mediators that achieved some success in the older dye sensitized literature also involve two-electron transfer.<sup>31</sup> Significantly, it has been known for some time that the reaction of aqueous Ti(III) ions with I<sub>3</sub><sup>-</sup> is also kinetically sluggish with an activation energy of 80 kcal/mol, Reaction 3.<sup>32</sup> Interestingly, this molecular analogue to the interfacial Reaction 2 is known to be catalyzed by redox active compounds and by interactions with Lewis bases.<sup>33–36</sup> Never-

- (12) Wang, X.; Stanbury, D. M. *Inorg. Chem.* **2006**, *45*, 3415.  
 (13) Bergeron, B. V.; Meyer, G. J. *J. Phys. Chem. B* **2003**, *107*, 245.  
 (14) Crutchley, R. J.; Lever, A. B. P. *Inorg. Chem.* **1982**, *21*, 2276.  
 (15) Crutchley, R. J.; Lever, A. B. P.; Poggi, A. *Inorg. Chem.* **1983**, *22*, 2647.  
 (16) Kalyanasundaram, K. *Photochemistry of Polypyridine and Porphyrin Complexes*; Academic Press: Suffolk, 1992.  
 (17) Hagfeldt, A.; Grätzel, M. *Acc. Chem. Res.* **2000**, *33*, 269.  
 (18) Hagfeldt, A.; Grätzel, M. *Chem. Rev.* **1995**, *95*, 49.

- (19) Ardo, S.; Meyer, G. J. *Chem. Soc. Rev.* **2009**, *38*, 115.  
 (20) Reynal, A.; Forneli, A.; Martinez-Ferrero, E.; Sanchez-Diaz, A.; Vidal-Ferran, A.; O'Regan, B. C.; Palomares, E. *J. Am. Chem. Soc.* **2008**, *130*, 13558.  
 (21) O'Regan, B. C.; Lopez-Duarte, I.; Martinez-Diaz, M. V.; Forneli, A.; Albero, J.; Morandeira, A.; Palomares, E.; Torres, T.; Durrant, J. R. *J. Am. Chem. Soc.* **2008**, *130*, 2906.  
 (22) O'Regan, B. C.; Walley, K.; Juozapavicius, M.; Anderson, A.; Matar, F.; Ghaddar, T.; Zakeeruddin, S. M.; Klein, C.; Durrant, J. R. *J. Am. Chem. Soc.* **2009**, *131*, 3541.  
 (23) Clark, C. C.; Meyer, G. J.; Wei, Q.; Galoppini, E. *J. Phys. Chem. B* **2006**, *110*, 11044.  
 (24) Green, A. N. M.; Chandler, R. E.; Haque, S. A.; Nelson, J.; Durrant, J. R. *J. Phys. Chem. B* **2005**, *109*, 142.  
 (25) Saveant, J. M. *Acc. Chem. Res.* **1993**, *26*, 455.  
 (26) Sapp, S. A.; Elliott, C. M.; Contado, C.; Caramori, S.; Bignozzi, C. A. *J. Am. Chem. Soc.* **2002**, *124*, 11215.  
 (27) Brugnati, M.; Caramori, S.; Cazzanti, S.; Marchini, L.; Argazzi, R.; Bignozzi, C. A. *Int. J. Photoenergy* **2007**, 80756–80766.  
 (28) Bergeron, B. V.; Marton, A.; Oskam, G.; Meyer, G. J. *J. Phys. Chem. B* **2005**, *109*, 937.  
 (29) Bhattacharya, S.; Kundu, K. K. *Bull. Chem. Soc. Jpn.* **1989**, *62*, 2676.  
 (30) Datta, J.; Bhattacharya, A.; Kundu, K. K. *Bull. Chem. Soc. Jpn.* **1988**, *61*, 1735.  
 (31) Desilvestro, J.; Graetzel, M.; Kavan, L.; Moser, J.; Augustynski, J. *J. Am. Chem. Soc.* **1985**, *107*, 2988.  
 (32) Xiao, S. R.; Spiro, M. J. *Chem. Soc. Faraday Trans.* **1994**, *90*, 1983.

theless, the uncertainties and speculation described here and elsewhere in the literature underscore the need for fundamental studies of  $I^-/I_3^-$  redox chemistry in nonaqueous solution.



In a recent communication, kinetic evidence was presented for the oxidation of iodide by the metal-to-ligand charge transfer (MLCT) excited state of  $\text{Ru}(\text{bpz})_2(\text{deeb})^{2+}$ .<sup>9</sup> Herein additional mechanistic details of excited state and thermal electron transfer reactions relevant to this and the subsequent formation and breaking of I–I bonds are described. In comparative studies, iodine atoms were photogenerated under similar experimental conditions by the direct excitation of  $\text{I}_3^-$ . In the presence of excess iodide, the iodine atoms were found to form I–I chemical bonds analogously to those generated by MLCT excited states. Unwanted dissociative electron transfer reactions that break the photogenerated chemical bonds and reform ground state products were also characterized. The possible relevance of this fundamental research to solar energy conversion and storage is discussed.

## Experimental Section

**Materials.** Tetrabutylammonium iodide, TBAI (Fluka, >98%), tetrabutylammonium tri-iodide,  $\text{TBAI}_3$  (Fluka, >97%),  $[\text{Ru}(\text{bpy})_3]\text{Cl}_2 \cdot 6\text{H}_2\text{O}$  (Aldrich, 99.95%), acetonitrile (Burdick & Jackson, spectrophotometric grade), ethanol (Warner-Graham, 200 proof anhydrous), methanol (Fisher, spectrophotometric grade), and triethanolamine, TEA (Fisher, 99.9%) were used as received.  $[\text{Ru}(\text{bpz})_2(\text{deeb})](\text{PF}_6)_2$  was prepared following established methods.<sup>13</sup>

**Steady State Absorption.** UV–vis absorption spectra were obtained on a Varian Cary 50 UV–vis spectrophotometer at room temperature. The extinction coefficients for  $\text{I}_3^-$ ,  $\text{I}^-$ , and  $\text{Ru}(\text{bpz})_2(\text{deeb})^{2+}$  in acetonitrile were determined spectroscopically through Beer's Law analysis of solutions of known concentration. The extinction coefficient for  $\text{I}_3^-$  was corrected for the equilibrium with  $\text{I}^-$  and  $\text{I}_2$ . The extinction coefficient for  $\text{Ru}(\text{bpz})_2(\text{deeb})^{2+}$  was calculated following an established literature method; photolysis of  $\text{Ru}(\text{bpz})_2(\text{deeb})^{2+}$  in the presence of 300 mM TEA.<sup>6</sup> All solutions were purged with argon prior to experiments.

**Nanosecond Transient Absorption.** Samples were excited by a pulsed Nd:YAG laser (BigSky Brilliant B, 8 ns fwhm, 1 Hz) tuned to 532 or 355 nm with appropriate optics. A pulsed 150 W xenon arc lamp (Applied Photophysics) served as the probe beam and was aligned perpendicular to the laser excitation light. Detection was achieved with a monochromator (Spex 1702/04) optically coupled to an R928 photomultiplier tube (Hamamatsu). Transient data was acquired on a computer-interfaced digital oscilloscope (LeCroy 9450, Dual 350 MHz) every 5 nm between 375 and 800 nm. Typically, 40–100 laser pulses were averaged at each observation wavelength. The excitation irradiance, 355 or 532 nm, was measured by a thermopile power meter (Moletron). The instrument response time was  $\sim 10$  ns.

**Comparative Actinometry.** For 532 nm excitation,  $[\text{Ru}(\text{bpy})_3]\text{Cl}_2$  in water was used as a relative actinometer for cage escape yield measurements. The difference between the ground state and excited state extinction coefficient was taken to be  $10\,000 \text{ M}^{-1} \text{ cm}^{-1}$  at 450 nm and the intersystem crossing yield was assumed to be unity. For 355 nm excitation, 9,10-dibromoanthracene in toluene was used as an actinometer. The intersystem crossing yield was taken to be 0.7 and the extinction coefficient at 427.5 nm was

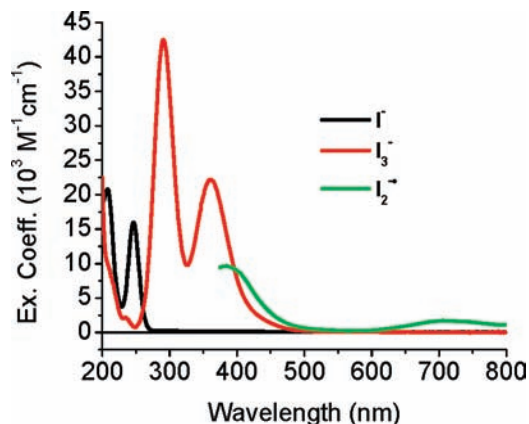


**Figure 1.** UV–vis absorption spectra of TBAI,  $\text{TBAI}_3$ , and the iodine radical anion ( $\text{I}_2^{\bullet-}$ ) in acetonitrile.

$48\,000 \text{ M}^{-1} \text{ cm}^{-1}$ .<sup>37</sup> The concentration of  $\text{I}_2^{\bullet-}$  was quantified at 710 nm where the extinction coefficient was  $1700 \text{ M}^{-1} \text{ cm}^{-1}$ .

**Steady State Photoluminescence.** A Spex Fluorolog with a 450 W Xe lamp was utilized for steady state photoluminescence (PL) measurements. PL spectra were acquired at room temperature of micromolar  $\text{Ru}(\text{bpz})_2(\text{deeb})(\text{PF}_6)_2$  argon purged acetonitrile solutions and at 77K in a 4:1 *v:v* ethanol:methanol glass. At room temperature the PL quantum yield was calculated by the comparative method with  $[\text{Ru}(\text{bpy})_3]\text{Cl}_2$  in argon purged water as the actinometer.<sup>38</sup>

**Time Resolved Photoluminescence.** Temperature dependent nanosecond time-resolved PL data were acquired at a right angle to excitation with pulsed 500 nm laser light from a  $\text{N}_2$  dye laser (Photon Technologies International, GL301, Coumarin 500 (Exciton)). Transient data was digitized on a computer-interfaced oscilloscope (LeCroy LT322). A methanol bath circulator (Thermo) controlled the sample temperature from 240–290 K in an insulated cuvette holder.

**Photochemical Ligand Loss.** The photostability of  $\text{Ru}(\text{bpz})_2(\text{deeb})(\text{PF}_6)_2$  toward ligand loss was quantified in argon purged acetonitrile solutions with  $30 \mu\text{M}$   $\text{Ru}(\text{bpz})_2(\text{deeb})(\text{PF}_6)_2$  and 10 mM TBAI. This solution was photolyzed continually for 5 h with 488 nm light ( $3.0 \text{ mW/cm}^2$  Coherent  $\text{Ar}^+$  ion laser) and steady state absorbance spectra were taken at regular intervals. The incident irradiance was measured with a calibrated silicon photodiode and the concentration changes were calculated with Beer's Law. Steady-state 488 nm light excitation of  $\text{Ru}(\text{bpz})_2(\text{deeb})(\text{PF}_6)_2$  in the presence of 0.5 M TBAI solutions resulted in spectral features that were consistent with the loss of a diimine ligand and the formation of  $\text{Ru}^{\text{II}}(\text{bpz})(\text{L}')(\text{CH}_3\text{CN})(\text{I})^+$ , where  $\text{L}' = \text{bpz}$  or  $\text{deeb}$ .<sup>14,15</sup> Absorbance spectra measured pre- and post- photolysis showed growths centered at 385 and 500 nm that tailed into the UV and near-IR respectively as well as a bleach between isosbestic points at 413 and 464 nm. The isosbestic points were maintained throughout the photolysis, consistent with production of a single photoproduct. The quantum yield was determined to be  $\phi = 5 \pm 2 \times 10^{-5}$ , from the initial loss of  $\text{Ru}(\text{bpz})_2(\text{deeb})(\text{PF}_6)_2$ .

## Results

Tri-iodide had two absorption bands in the ultraviolet region in about a 2:1 ratio with maxima at 291 nm ( $\epsilon = 42\,500 \text{ M}^{-1} \text{ cm}^{-1}$ ) and 361 nm ( $\epsilon = 22\,200 \text{ M}^{-1} \text{ cm}^{-1}$ ) in acetonitrile at room temperature. Iodide had an absorption maxima at 208 nm ( $\epsilon = 20\,800 \text{ M}^{-1} \text{ cm}^{-1}$ ) and 246 nm ( $\epsilon = 16\,300 \text{ M}^{-1} \text{ cm}^{-1}$ ). The absorption spectrum of the tetrabutyl ammonium salts are shown in Figure 1 and this cation was used exclusively in these studies.

(33) Koval, C. A.; Drew, S. M. *Inorg. Chem.* **1988**, *27*, 4323.

(34) Johnson, C. E.; Winstein, S. *J. Am. Chem. Soc.* **1952**, *74*, 755.

(35) Johnson, C. E.; Winstein, S. *J. Am. Chem. Soc.* **1952**, *74*, 3105.

(36) Johnson, C. E.; Winstein, S. *J. Am. Chem. Soc.* **1951**, *73*, 2601.

(37) Darmanyan, A. P. *Chem. Phys. Lett.* **1984**, *110*, 89.

(38) Crosby, G. A.; Demas, J. N. *J. Phys. Chem.* **1971**, *75*, 991.



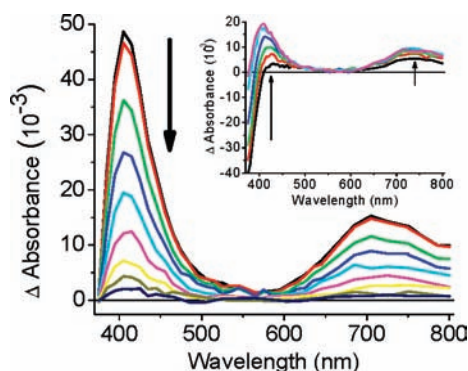


**Figure 2.** Transient absorbance spectra after pulsed 355 nm light excitation of 10  $\mu\text{M}$  TBAI<sub>3</sub> and 1 mM TBAI in argon-purged acetonitrile observed 100 ns to 1 ms. (Inset) Transient absorbance spectra of 23  $\mu\text{M}$  TBAI<sub>3</sub> and 30  $\mu\text{M}$  TBAI in argon-purged acetonitrile collected 100 ns to 10.0  $\mu\text{s}$  after laser excitation. The arrows show the direction of the absorption change.

Nanosecond transient absorption was used to characterize intermediates observed after pulsed laser excitation of tri-iodide ions in argon-purged acetonitrile solutions. The observed kinetics, spectra, and photostability were found to be dependent on the concentration of iodide present in the I<sub>3</sub><sup>-</sup> acetonitrile containing solution. In the absence of intentionally added iodide, irreversible photochemistry was observed as a decrease in tri-iodide and an increase in iodide concentration. This photochemistry precluded signal averaging but was absent when significant concentrations of TBAI were present in the acetonitrile solution. Therefore, all quantitative time-resolved spectroscopic studies were performed in the presence of intentionally added iodide.

With 4  $\mu\text{M}$  to 1 mM iodide and 10–30  $\mu\text{M}$  tri-iodide no permanent photochemistry was observed after pulsed 355 or 532 nm laser excitation of I<sub>3</sub><sup>-</sup>. An intermediate was observed that consisted of a bleach of the tri-iodide absorption and a positive absorption with a maximum  $\sim$ 750 nm, Figure 2 inset. The intermediate was reasonably assigned to the iodine radical anion, I<sub>2</sub><sup>-•</sup>, based on the known spectrum in water. A biphasic absorption change was observed across the visible region. A positive absorption was observed at  $\lambda > 400$  nm within the instrument response time,  $k > 10^8$  s<sup>-1</sup>, followed by a slower growth of equal amplitude within experimental uncertainty. The kinetics of this slower component were found to be iodide concentration dependent, while the initial response was not. Representative data are shown in Figure 3. The observed rate constant for the slower component increased linearly with iodide concentration from which a second-order rate constant of  $k = 2.5 \pm 0.4 \times 10^{10}$  M<sup>-1</sup> s<sup>-1</sup> was abstracted, Figure 3 inset. The absorption change associated with I<sub>2</sub><sup>-•</sup> decayed to zero at all observation wavelengths in good agreement with a second-order equal concentration kinetic model,  $k = 3.3 \pm 0.1 \times 10^9$  M<sup>-1</sup> s<sup>-1</sup>. At greater than millimolar iodide concentrations, the slower component could not be time-resolved and the observed spectrum no longer showed the tri-iodide bleach, Figure 2. The transient absorption spectra were satisfactorily modeled as the loss of one tri-iodide and formation of two I<sub>2</sub><sup>-•</sup>. The two I<sub>2</sub><sup>-•</sup> produced absorb light more strongly than does I<sub>3</sub><sup>-</sup> so that only positive absorption changes were observed. From the tri-iodide extinction coefficient and this transient spectral data, the extinction coefficient and absorption spectrum of I<sub>2</sub><sup>-•</sup> in acetonitrile was calculated, Figure 1.

The visible absorbance spectrum of Ru(bpz)<sub>2</sub>(deeb)(PF<sub>6</sub>)<sub>2</sub> in acetonitrile solution showed the expected MLCT absorption

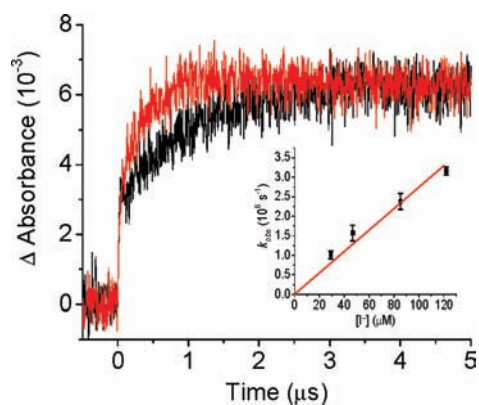


**Figure 3.** Time resolved absorption change measured at 705 nm after pulsed 355 nm excitation of I<sub>3</sub><sup>-</sup> in 30  $\mu\text{M}$  (black) and 160  $\mu\text{M}$  (red) TBAI acetonitrile solution. (Inset) Plot of the observed first-order rate constants as a function of the iodide concentration.

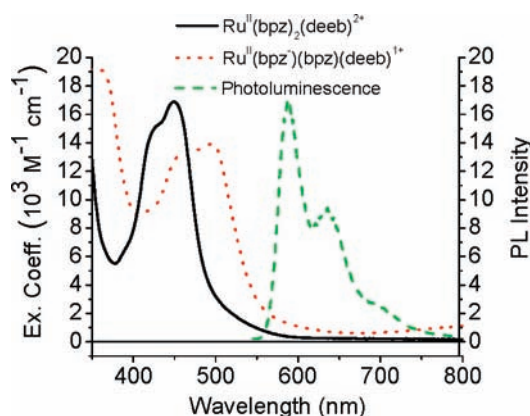


**Figure 4.** Absorption spectrum of Ru(bpz)<sub>2</sub>(deeb)<sup>2+</sup> (solid line) and Ru(bpz<sup>-</sup>)(bpz)(deeb)<sup>+</sup> (dotted line) in acetonitrile. Steady state photoluminescence spectrum of Ru(bpz)<sub>2</sub>(deeb)<sup>2+</sup> measured at 77 K in a 4:1 ethanol:methanol glass (dashed line) with 450 nm light excitation.

band maximum at 450 nm, Figure 4. Steady state photolysis of Ru(bpz)<sub>2</sub>(deeb)<sup>2+</sup> in the presence of triethanolamine resulted in a solution color change from bright yellow to red; the absorption at 450 nm decreased with a new maximum at 496 nm, a strong absorbance in the near-UV, and a weak broad peak in the near-IR, attributed to the reduced dye, Ru(bpz<sup>-</sup>)(bpz)(deeb)<sup>+</sup>, Figure 4. Isosbestic points were maintained over the course of the photolysis at 404 and 465 nm. Upon exposure to air the absorption spectrum of Ru(bpz)<sub>2</sub>(deeb)<sup>2+</sup> was quantitatively recovered.

The room temperature steady state photoluminescence spectrum of Ru(bpz)<sub>2</sub>(deeb)<sup>2+</sup> in argon-purged acetonitrile solution was broad and unstructured with a maximum intensity centered around 620 nm. The quantum yield was estimated to be 0.14 with an excited state lifetime of 1.75  $\mu\text{s}$  from which radiative and nonradiative rate constants  $k_r = 8.36 \times 10^4$  s<sup>-1</sup> and  $k_{nr} = 5.01 \times 10^5$  s<sup>-1</sup> were abstracted. In a 4:1 ethanol:methanol glass at 77 K, the Ru(bpz)<sub>2</sub>(deeb)<sup>2+</sup> photoluminescence spectrum was blue-shifted with maximum intensity around 590 nm and a well resolved vibronic structure, with a  $\sim$ 1300 cm<sup>-1</sup> quantum spacing, Figure 4.

The temperature dependence of the excited state lifetime was quantified in acetonitrile from 240–290 K. Excited state decay was well described by a first-order kinetic model over the whole temperature region investigated, and the lifetimes decreased as

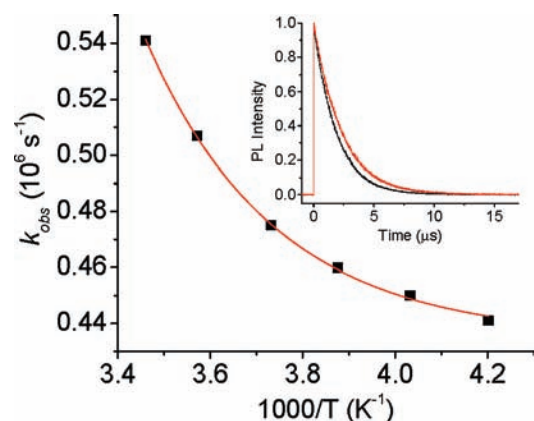


**Figure 5.** First-order rate constants for excited state decay in acetonitrile versus  $1000/T$  (black dots). Overlaid on this data is a best fit to a modified Arrhenius equation (red line);  $E_a = 2.5 \pm 0.1 \times 10^3 \text{ cm}^{-1}$  and  $A = 2 \pm 1 \times 10^{10} \text{ s}^{-1}$ . (Inset) Excited state decay measured at 289 (black) and 238 (red) K.

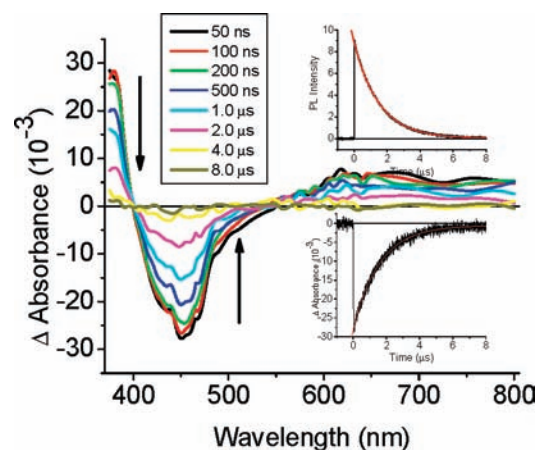


**Figure 6.** Time resolved absorbance difference spectra recorded at the indicated delay times after pulsed 532 nm excitation of  $\text{Ru}(\text{bpz})_2(\text{deeb})(\text{PF}_6)_2$  in acetonitrile. (Inset above) PL decay monitored at 620 nm. (Inset below) Excited state bleach measured at 450 nm. Overlaid on both insets are fits to a first-order kinetic model.

the temperature increased, Figure 5. The data was fit to a modified Arrhenius equation<sup>39</sup> from which an activation energy and pre-exponential factor were abstracted,  $E_a = 2.5 \pm 0.1 \times 10^3 \text{ cm}^{-1}$ ,  $A = 2 \pm 1 \times 10^{10} \text{ s}^{-1}$ .

Pulsed 532 nm light excitation of  $\text{Ru}(\text{bpz})_2(\text{deeb})^{2+}$  in argon purged acetonitrile resulted in the appearance of the absorption difference spectra shown in Figure 6. A bleach of the ground state MLCT absorption at  $\sim 450 \text{ nm}$  and excited state absorbances in the near-UV and red to near-IR regions were observed with isosbestic points at 400 and 540 nm. The transient absorbance change monitored at 450 nm and time-resolved photoluminescence collected at 620 nm were first-order and yielded equivalent rate constants with no measurable photochemistry, Figure 6 insets.

The addition of iodide to an argon saturated acetonitrile solution of  $\text{Ru}(\text{bpz})_2(\text{deeb})(\text{PF}_6)_2$  was found to decrease the excited state lifetime, Figure 7. There was no significant change in the visible absorbance spectrum or in the initial amplitude of the photoluminescence decays with added iodide. The iodide

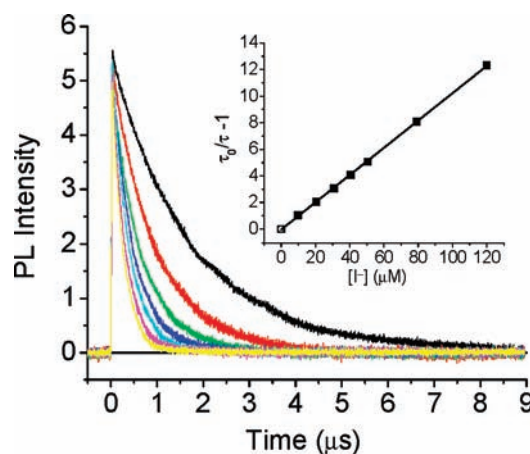


**Figure 7.** Photoluminescence decays measured after pulsed 532 nm excitation of  $\text{Ru}(\text{bpz})_2(\text{deeb})^{2+}$  in acetonitrile with 0 to 120  $\mu\text{M}$  TBAI. The inset shows Stern–Volmer plot of this same data from which  $K_{\text{SV}} = 1.1 \pm 0.1 \times 10^5 \text{ M}^{-1}$  and  $k_q = 6.6 \pm 0.3 \times 10^{10} \text{ M}^{-1} \text{ s}^{-1}$  were abstracted.

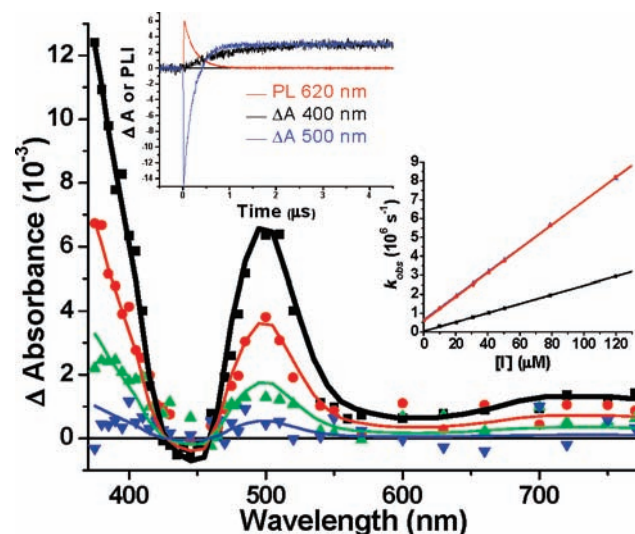


**Figure 8.** Absorption difference spectra measured at 1  $\mu\text{s}$  (■), 50  $\mu\text{s}$  (▼), and 1 ms (▼) under conditions identical to that in Figure 6 except in the presence of 500 mM iodide. The upper inset shows absorption and PL intensity changes monitored at the indicated wavelengths after excitation of 14  $\mu\text{M}$   $\text{Ru}(\text{bpz})_2(\text{deeb})^{2+}$  in 58  $\mu\text{M}$  TBAI. The inset on the right shows a plot of the first order rate constants for the formation of  $\text{I}_2^{\bullet-}$  (■) and  $\text{Ru}(\text{bpz})(\text{bpz})(\text{deeb})^+$  (▲) and the excited state lifetime,  $\tau$ , as a function of iodide concentration.

quenching was found to follow the Stern–Volmer model, eq 4 and Figure 7 inset. A Stern–Volmer constant

$$\tau_0/\tau = 1 + K_{\text{sv}}[\text{I}] \quad (4)$$

$K_{\text{sv}} = 1.1 \pm 0.1 \times 10^5 \text{ M}^{-1}$  was abstracted from the slope with a dynamic quenching rate constant  $k_q = 6.6 \pm 0.3 \times 10^{10} \text{ M}^{-1} \text{ s}^{-1}$ , where  $k_q = K_{\text{sv}}/\tau_0$ .

Pulsed laser excitation under conditions identical to that in Figure 6 except in the presence of 500 mM TBAI, led to the appearance of new transient absorption features that were well described by equal concentrations of  $\text{Ru}(\text{bpz})(\text{bpz})(\text{deeb})^+$  and  $\text{I}_2^{\bullet-}$ , Figure 8. The 500 nm absorption band was assigned to the reduced ruthenium compound. The absorption with  $\lambda < 400 \text{ nm}$  and the weak red absorption were assigned to  $\text{I}_2^{\bullet-}$ . These assignments were made after comparisons with and simulations

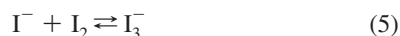
(39) Juris, A.; Balzani, V.; Barigelletti, F.; Campagna, S.; Belser, P.; Von Zelewsky, A. *Coord. Chem. Rev.* **1988**, *84*, 85.

based on the authentic spectra shown in Figure 4. Excited state quenching was quantitative but the yield of charge separated products was low. Comparative actinometry with Ru(bpy)<sub>3</sub><sup>2+</sup> as a reference was used to quantify the yield of products present 10 ns after the laser excitation,  $\phi_{CE} = 0.042 \pm 0.001$ .

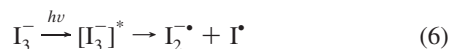
At lower iodide concentrations (<1 mM), the appearance of the electron transfer products was quantified with nanosecond time resolution. Shown in the right inset of Figure 8 are first-order rate constants measured as a function of the iodide concentration. Excited state relaxation was monitored by photoluminescence, and the formation of the reduced compound by transient absorption at 500 nm. The formation of I<sub>2</sub><sup>-•</sup> was monitored at 400 nm which is an isosbestic point between the ground and excited state and is very close to a ground-reduced state isosbestic point. The formation and decay of I<sub>2</sub><sup>-•</sup> could therefore be quantified at this wavelength without interference from other solution species, Figure 8 upper inset. A second-order rate constant for I<sub>2</sub><sup>-•</sup> formation was abstracted from iodide concentration dependent kinetic data like that shown,  $k_1 = 2.4 \pm 0.2 \times 10^{10} \text{ M}^{-1} \text{ s}^{-1}$ . The formation of the reduced compound was monitored at 500 nm and was found to appear with the same rate constant as excited state decay,  $k = 6.6 \pm 0.3 \times 10^{10} \text{ M}^{-1} \text{ s}^{-1}$ , Figure 8 inset. Recombination to yield ground state products was well described by a second-order equal concentration kinetic model,  $k_{cr} = 2.1 \pm 0.3 \times 10^{10} \text{ M}^{-1} \text{ s}^{-1}$ .

## Discussion

**A. I<sub>3</sub><sup>-</sup> Photochemistry.** Relevant to the solution photochemistry of tri-iodide ion is the equilibrium with iodine and iodide, reaction 5.<sup>1</sup> The equilibrium constant in acetonitrile is much larger than that in water,  $K = 6 \pm 2 \times 10^6 \text{ M}^{-1}$  versus  $740 \text{ M}^{-1}$ , behavior attributed to the ability of iodide to more effectively compete with solvent for the open coordination sites on I<sub>2</sub>.<sup>40,41</sup>



Visible or ultraviolet light excitation of tri-iodide resulted in the rapid formation of the iodine radical anion, I<sub>2</sub><sup>-•</sup>, and the iodine atom. The I<sub>3</sub><sup>-\*</sup> excited state was not observed due to its subpicosecond lifetime and dissociative nature.<sup>42–45</sup> Likewise the iodine atom was not observed spectroscopically but compelling kinetic evidence for its presence was found.



The quantum yield for reaction 6, measured by comparative actinometry, was found to be 0.6 which is over a factor of 2 larger than the value reported in aqueous solution.<sup>42</sup> The fate of the 40% of I<sub>3</sub><sup>-\*</sup> that did not yield long-lived I<sup>•</sup> and I<sub>2</sub><sup>-•</sup> redox products is unknown. Room temperature photoluminescence has been reported for I<sub>3</sub><sup>-\*</sup> in ethanol but was not observed in acetonitrile nor were any long-lived excited states,  $\tau > 10 \text{ ns}$ .<sup>46</sup>

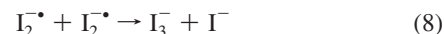
As no other products were observed, the 40% of absorbed photons that did not yield long-lived redox states are tentatively attributed to photodissociation followed by geminate bond reformation within the solvent cage to yield I<sub>3</sub><sup>-</sup>.

Pulsed laser excitation of I<sub>3</sub><sup>-</sup> in acetonitrile was accompanied by permanent photochemistry manifest as a loss in tri-iodide and an increase in the iodide concentration. However, when iodide was intentionally added to the TBAI<sub>3</sub> solution, no net photochemistry was observed. The added iodide is presumed to quantitatively react with the photogenerated iodine atoms to yield I<sub>2</sub><sup>-•</sup>, reaction 7. Therefore, two I<sub>2</sub><sup>-•</sup> were produced for each absorbed photon that led to I<sub>3</sub><sup>-</sup> bond cleavage with an effective quantum yield of 1.2, reactions 6 and 7.

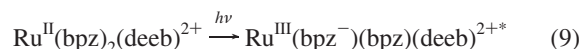


At low I<sup>-</sup> concentrations, the formation of the second equivalent of I<sub>2</sub><sup>-•</sup> formed by reaction 7 was time-resolved,  $k = 2.5 \pm 0.4 \times 10^{10} \text{ M}^{-1} \text{ s}^{-1}$ . This rate constant was within experimental uncertainty the same as the previously reported literature value,  $2.3 \times 10^{10} \text{ M}^{-1} \text{ s}^{-1}$ , and was about twice as large as the published aqueous value,  $8.8 \times 10^9 \text{ M}^{-1} \text{ s}^{-1}$ .<sup>47,48</sup>

The extinction coefficient and absorption spectrum of I<sub>2</sub><sup>-•</sup> in acetonitrile were calculated to have maxima at 385 nm ( $\epsilon = 9700 \text{ M}^{-1} \text{ cm}^{-1}$ ) and  $710 \pm 5 \text{ nm}$  ( $\epsilon = 1700 \text{ M}^{-1} \text{ cm}^{-1}$ ) in reasonable agreement with aqueous data.<sup>47,49</sup> The I<sub>2</sub><sup>-•</sup> was only transiently formed and returned to ground state products by a second-order equal concentration kinetic pathway, reaction 8. The second-order rate constant for this disproportionation reaction was calculated to be  $3.3 \pm 0.1 \times 10^9 \text{ M}^{-1} \text{ s}^{-1}$ , that is within experimental error of literature values measured in water  $3 \pm 1 \times 10^9 \text{ M}^{-1} \text{ s}^{-1}$ .<sup>47,49</sup>



**B. MLCT Excited State.** The photophysical properties of Ru(bpz)<sub>2</sub>(deeb)<sup>2+</sup> are typical of metal-to-ligand charge transfer (MLCT) excited states and therefore are only briefly described.<sup>39</sup> A comparison of the excited state absorption spectra of Ru(bpz)<sub>2</sub>(deeb)<sup>2+</sup>, Ru(deeb)<sub>3</sub><sup>2+</sup> and Ru(bpy)<sub>2</sub>(deeb)<sup>2+</sup> indicate that the excited state is localized on the bipyrazine ligand, eq 9.<sup>50,51</sup> This assignment is also consistent with the proposal that the first diimine ligand reduced electrochemically in heteroleptic Ru(II) compounds is also the ligand that the excited state will localize upon in the equilibrated excited state.<sup>39</sup>



The excited state was emissive with a notably high quantum yield for room temperature photoluminescence,  $\phi = 0.14$  that emanates from a smaller nonradiative rate constant than expected for an orange emitter,  $k_{nr} = 5.01 \pm 0.02 \times 10^5 \text{ s}^{-1}$ . The introduction of conjugated substituents in the 4 and 4' positions of bipyridine, such as olefins or aromatic groups or like the esters utilized here, are known to enhance excited state

(40) Barraqué, C.; Vedel, J.; Trémillon, B. *Anal. Chim. Acta* **1969**, *46*, 263.

(41) Crawford, E.; McIndoe, J. S.; Tuck, D. G. *Can. J. Chem.* **2006**, *84*, 1607.

(42) Gershgoren, E.; Banin, U.; Ruhman, S. *J. Phys. Chem. A* **1998**, *102*, 9.

(43) Kühne, T.; Küster, R.; Vöhringer, P. *Chem. Phys.* **1998**, *233*, 161.

(44) Kühne, T.; Vöhringer, P. *J. Chem. Phys.* **1996**, *105*, 10788.

(45) Behar, D.; Rabani, J. *J. Phys. Chem. B* **2001**, *105*, 6324.

(46) Gilch, P.; Hartl, I.; An, Q.; Zinth, W. *J. Phys. Chem. A* **2002**, *106*, 1647.

(47) Elliot, A. J. *Can. J. Chem.* **1992**, *70*, 1658.

(48) Treinin, A.; Hayon, E. *Int. J. Radiat. Phys. Chem.* **1975**, *7*, 387.

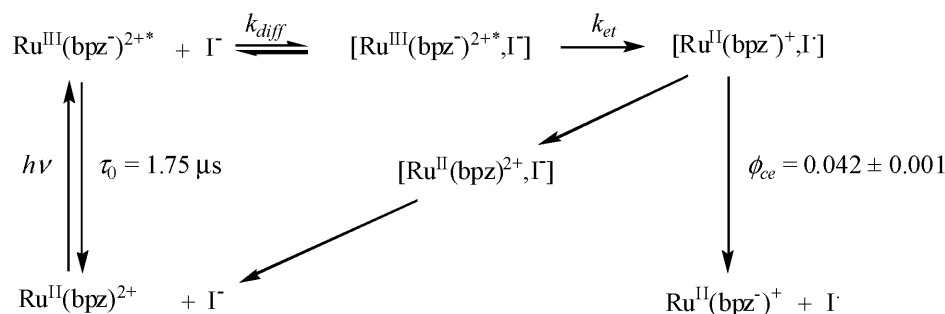
(49) Grossweiner, L. I.; Matheson, M. S. *J. Phys. Chem.* **1957**, *61*, 1089.

(50) Gardner, J. M. Formation of Chemical Bonds with Visible Light: The Sensitized Oxidation of Iodide and Water, PhD Thesis, Johns Hopkins University, Baltimore, MD, 2009.

(51) Kelly, C. A.; Farzad, F.; Thompson, D. W.; Meyer, G. J. *Langmuir* **1999**, *15*, 731.



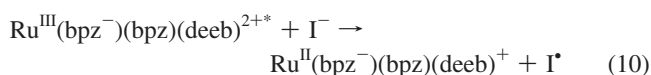
Scheme 2



lifetimes.<sup>52–57</sup> It is interesting that this enhancement is observed even though the excited state is localized on an adjacent bipyrazine ligand.

The weak temperature dependence of excited state relaxation was examined to establish the activated decay pathways of  $\text{Ru}^{\text{III}}(\text{bpz}^-)(\text{bpz})(\text{deeb})^{2+*}$ . Arrhenius analysis of the temperature dependent lifetimes revealed an activation energy of  $\sim 2500 \text{ cm}^{-1}$ , typical of MLCT excited states. The pre-exponential factor of  $10^{10} \text{ s}^{-1}$  is within the range reported in previous studies of Ru-bipyrazine excited states yet is somewhat lower than the  $10^{12}–10^{13} \text{ s}^{-1}$  usually reported for Ru(II)-polypyridine compounds.<sup>39</sup> Nevertheless, the data is consistent with the previous conclusion that the activated pathway involves surface crossing from the <sup>3</sup>MLCT state to a ligand field or an upper MLCT state.<sup>39,58</sup> Significantly, the rate constant for activated decay is on the order of  $1 \times 10^5 \text{ s}^{-1}$  indicating that about 20% of nonradiative excited state relaxation follows this pathway at room temperature. At first glance this seems inconsistent with the much lower,  $5 \times 10^{-5}$ , quantum yield for photochemical ligand loss as the ligand field state is antibonding with respect to metal–ligand bonds. This quantum yield is significantly smaller than that reported for  $\text{Ru}(\text{bpz})_3^{2+*}$ ,  $\Phi_{\text{LL}} > 0.001$ .<sup>14</sup> A reasonable explanation stems from the fact that iodide is an efficient excited state quencher and at 10 mM concentration, the excited state lifetime is only  $\sim 60 \text{ ns}$ . Therefore, fast electron transfer from iodide to the excited state increases the stability of  $\text{Ru}(\text{bpz})_2(\text{deeb})^{2+}$  toward photochemical ligand loss.

**C. Excited State Hole Transfer.** The MLCT excited state of  $\text{Ru}(\text{bpz})_2(\text{deeb})^{2+}$  was quenched by iodide in  $\text{CH}_3\text{CN}$ . A Stern–Volmer constant of  $1.1 \pm 0.1 \times 10^5 \text{ M}^{-1}$  was abstracted that corresponds to a quenching rate constant of  $6.6 \pm 0.3 \times 10^{10} \text{ M}^{-1} \text{ s}^{-1}$ . Significantly, the measured rate constants for excited state decay and for appearance of the reduced ruthenium product were the same. However, the reduced ruthenium compound appeared about a factor of 3 faster than did  $\text{I}_2^{\cdot-}$  indicating that the iodine radical anion was a secondary photochemical product. Indeed  $\text{I}_2^{\cdot-}$  formed with the same rate constant as that measured after pulsed excitation of  $\text{I}_3^-$  (Reaction 9), providing evidence that the iodine atom was the primary product responsible for excited state reductive quenching, Reaction 10.



Since the formal oxidation state of Ru in the MLCT excited state is III, this reaction can also be viewed as “hole” transfer from a Ru  $t_{2g}$  orbital to an iodide p orbital. This viewpoint would be most accurate if hole transfer from the initially formed (Franck–Condon) excited state was relevant, eq 9. Configurational

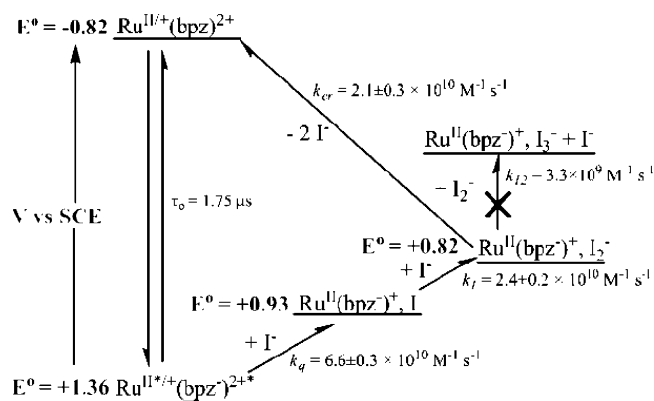
mixing accompanies excited state relaxation to equilibrated MLCT excited state such that the “hole” occupies molecular orbitals with significant diimine character. In fact, quantum mechanical calculations of  $\text{Ru}(\text{bpy})_3^{2+}$  indicate significantly less than the unit increase in the Ru formal oxidation state implied in eq 9.<sup>59</sup> Similar behavior is expected for  $\text{Ru}^{\text{III}}(\text{bpz}^-)(\text{bpz})(\text{deeb})^{2+*}$ , as bipyrazine is at least as strong a  $\pi$  acid as bipyridine even though it is a significantly weaker  $\sigma$ -donor.<sup>60</sup> Therefore, formal oxidation states should be regarded with care as there is expected to be significant metal and diimine character in the MLCT excited state hole transfer process, reaction 10.

Bimolecular excited state reactions are often found to obey two general mechanisms.<sup>61</sup> *Static* mechanisms involve the formation of nonphotoluminescent ground state donor–acceptor adducts. While there was no evidence for static electron transfer processes in this work, adduct formation between iodide and Ru(II) compounds have previously been observed in the solid state and in solution.<sup>7,8,11</sup> A *dynamic* mechanism involves diffusional encounters of the excited state and the redox active quencher prior to electron transfer.

Scheme 2 shows key steps relevant to the dynamic hole transfer studied here. A bpz and a deeb ligand were removed for clarity. Diffusional encounters of iodide and the MLCT excited state result in formation of an encounter complex with a well-defined cage of oriented dipoles and ions within which multiple collisional encounters can occur. The electron transfer products may either diffuse out of the cage or recombine to yield the excited state or ground state products. Back electron transfer to reform the excited state was not included here as excited state hole transfer was highly favored and occurred with a rate constant near the value expected for diffusion limited reactivity in acetonitrile at room temperature.

- (52) Wang, P.; Klein, C.; Humphry-Baker, R.; Zakeeruddin, S. M.; Gratzel, M. *J. Am. Chem. Soc.* **2005**, *127*, 808.
- (53) Chen, C. Y.; Wu, S. J.; Wu, C. G.; Chen, J. G.; Ho, K. C. *Angew. Chem., Int. Ed.* **2006**, *45*, 5822.
- (54) Jang, S. R.; Lee, C.; Choi, H.; Ko, J. J.; Lee, J.; Vittal, R.; Kim, K. J. *Chem. Mater.* **2006**, *18*, 5604.
- (55) Jiang, K. J.; Xia, J. B.; Masaki, N.; Noda, S.; Yanagida, S. *Inorg. Chim. Acta* **2008**, *361*, 783.
- (56) Karthikeyan, C. S.; Peter, K.; Wietasch, H.; Thelakkat, M. *Sol. Energy Mater. Sol. Cells* **2007**, *91*, 432.
- (57) Walters, K. A.; Premvardhan, L. L.; Liu, Y.; Peteanu, L. A.; Schanze, K. S. *Chem. Phys. Lett.* **2001**, *339*, 255.
- (58) Allen, G. H.; White, R. P.; Rillema, D. P.; Meyer, T. J. *J. Am. Chem. Soc.* **1984**, *106*, 2613.
- (59) Daul, C.; Baerends, E. J.; Vernooijs, P. *Inorg. Chem.* **1994**, *33*, 3538.
- (60) Gorelsky, S. I.; Dodsworth, E. S.; Lever, A. B. P.; Vlcek, A. A. *Coord. Chem. Rev.* **1998**, *174*, 469.
- (61) Lakowicz, J. R. *Principles of Fluorescence Spectroscopy*; Kluwer Academic/Plenum Publishers: New York, 1999.

## Scheme 3



The diffusion rate constant,  $k_{\text{diff}}$ , for two spherical neutral donors was calculated with eq 11.

$$k_{\text{diff}} = 4\pi N_A (D_{\text{I}^-} + D_{\text{Ru}^*}) \beta \quad (11)$$

The diffusion constant for iodide,  $D_{\text{I}^-}$ , was previously measured to be  $1.7 \times 10^{-9} \text{ m}^2 \text{ s}^{-1}$ ,<sup>62</sup> and a value of  $9.2 \times 10^{-10} \text{ m}^2 \text{ s}^{-1}$  was calculated by the Stokes–Einstein equation for  $D_{\text{Ru}^*}$ . For neutral compounds,  $\beta$  is the sum of the ionic radii, taken to be 7 Å for the Ru\* excited state and 2.2 Å for iodide. Calculation under these conditions yields  $k_{\text{diff}} = 1.82 \times 10^{10} \text{ M}^{-1} \text{ s}^{-1}$ .<sup>63–65</sup>

However, for diffusive ions charge must be taken into account and  $\beta$  was calculated by eq 12,

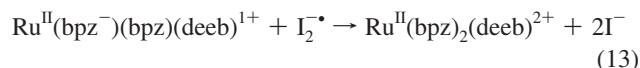
$$\beta = \frac{R_C}{\exp^{R_C/R} - 1} \quad (12)$$

where  $R$  is the sum of the ionic radii previously given,  $R_C$  is equal to  $[z_{\text{I}^-} z_{\text{Ru}^*} e^2 / 4\pi \epsilon_r \epsilon_0 k_B T]$ , where  $z$  is the ionic charge of iodide (−1), and the excited Ru compound (+2) and all the other variables have their usual meaning. The diffusion constant is thereby calculated as  $k_{\text{diff}} = 6.4 \times 10^{10} \text{ M}^{-1} \text{ s}^{-1}$  which was within experimental uncertainty of the measured excited state quenching rate constant and in good agreement with what has been calculated for similar systems.<sup>64</sup> The near coincidence of the measured quenching rate constant with the calculated diffusion constant indicates that hole transfer from the excited ruthenium compound to iodide is rate limited by diffusional encounters of the excited state and iodide, Scheme 2.

**D. Relevance to Solar Energy Conversion.** The kinetic and mechanistic information relevant to solar energy conversion are summarized in the Jablonski-type diagram shown in Scheme 3. The oxidizing power of the MLCT excited state was estimated by thermochemical cycles. A quasi-reversible wave for  $\text{Ru}^{2+/+}$  was reported at  $-0.82 \text{ V vs SCE}$ . The Gibbs free energy stored in the excited state was estimated from the onset of the corrected photoluminescence spectrum at 77 K,  $\Delta G_{\text{ES}} = 2.18 \text{ eV}$ . Taken together, this data indicates that  $\text{Ru}(\text{bpz})_2(\text{deeb})^{2+*}$  is a potent photo-oxidant capable of iodide and water oxidation,  $E^\circ(\text{Ru}^{2+*/+}) = +1.36 \text{ V vs SCE}$ .

Excited state hole transfer to yield the iodine atom is about 430 mV downhill and was previously discussed. Reaction of

the iodine atom with iodide to make an I–I bond lowers the free energy stored by 110 mV.<sup>8,17</sup> Therefore, the  $\text{Ru}(\text{bpz}^-)(\text{bpz})(\text{deeb})^+$ ,  $\text{I}_2^{\cdot-}$  charge separated state stores about 1.28 eV of energy for microseconds. Unwanted charge recombination to yield ground state products is highly thermodynamically favored ( $-\Delta G^\circ = 1.64 \text{ eV}$ ) and occurs with a rate constant of  $2.1 \times 10^{10} \text{ M}^{-1} \text{ s}^{-1}$ , reaction 13. Fessenden has proposed that the aqueous reduction of  $\text{I}_2^{\cdot-}$  by solvated



electrons occurs through an  $\text{I}_2^{\cdot-}$  intermediate.<sup>66</sup> There was no evidence for this or any other intermediates in acetonitrile. Also absent was  $\text{I}_2^{\cdot-}$  disproportionation chemistry that was observed after direct light excitation of  $\text{I}_3^-$ . The kinetic data shows that the reduced ruthenium compound competes efficiently for  $\text{I}_2^{\cdot-}$  and reacts almost ten times faster such that the disproportionation reaction can be ignored. This finding precluded studies of the potentially interesting reaction of  $\text{Ru}(\text{bpz}^-)(\text{bpz})(\text{deeb})^+$  with  $\text{I}_3^-$ .

Keeping in mind the fact that all the redox experiments reported herein were performed in fluid acetonitrile solution, the rapid reduction of  $\text{I}_2^{\cdot-}$  has interesting implications for dye sensitized solar cells. In attempts to increase the spectral sensitivity of the sensitizers to longer wavelengths, many researchers have utilized sensitizers with low-lying  $\pi^*$  orbitals.<sup>67–70</sup> Arakawa and co-workers found that such sensitizers have anomalously small open circuit photovoltages and can mediate the thermal reduction of the  $\text{I}^-/\text{I}_3^-$  electrolyte.<sup>67</sup> Similar behavior was reported by Bignozzi and co-workers for a series of black Os(II) sensitizers.<sup>68</sup> Indeed, it has also been found that Ru(II) and Os(II) compounds with coordinated 2,2'-biquinoline ligands can trap photoinjected electrons to yield the reduced compound.<sup>69–71</sup> Taken together, these observations suggested that an electron in the  $\pi^*$  orbitals of a coordinated diimine ligand can mediate unwanted charge recombination between  $\text{TiO}_2(e^-)$  and the redox active electrolyte. The data reported here shows that for the case of  $\text{I}_2^{\cdot-}$  acceptors, this reaction can be very fast.

The data reported here also raises the question of the possible relevance of iodine atoms to dye sensitized solar cells. While the competitive light absorption by tri-iodide has long been recognized to result in a measurable decrease in the photocurrent efficiency in the blue part of the visible region, the fact that the  $\text{I}_3^{\cdot-}$  produces iodine atoms with a quantum yield of 0.6 has not been acknowledged. In the high  $\sim 0.5 \text{ M}$  iodide acetonitrile solutions typically utilized in dye sensitized solar cells, the iodine atom product is expected to react quantitatively with iodide to yield the iodine radical anion that could in turn disproportionate such that no unwanted photochemistry occurs. The data reported here is consistent with this picture.

- (66) Nagarajan, V.; Fessenden, R. W. *J. Phys. Chem.* **1985**, *89*, 2330.  
 (67) Yanagida, M.; Yamaguchi, T.; Kurashige, M.; Hara, K.; Katoh, R.; Sugihara, H.; Arakawa, H. *Inorg. Chem.* **2003**, *42*, 7921.  
 (68) Altobello, S.; Argazzi, R.; Caramori, S.; Contado, C.; Da Fre, S.; Rubino, P.; Chone, C.; Larramona, G.; Bignozzi, C. A. *J. Am. Chem. Soc.* **2005**, *127*, 15342.  
 (69) Hoertz, P. G.; Thompson, D. W.; Friedman, L. A.; Meyer, G. J. *J. Am. Chem. Soc.* **2002**, *124*, 9690.  
 (70) Hoertz, P. G., Jr. Ph.D. Thesis, John Hopkins University, Baltimore, MD, 2003.  
 (71) Hoertz, P. G.; Staniszewski, A.; Marton, A.; Higgins, G. T.; Incarvito, C. D.; Rheingold, A. L.; Meyer, G. J. *J. Am. Chem. Soc.* **2006**, *128*, 8234.

- (62) Oskam, G.; Bergeron, B. V.; Meyer, G. J.; Searson, P. C. *J. Phys. Chem. B* **2001**, *105*, 6867.  
 (63) Steinfeld, J. L.; Francisco, J. S.; Hase, W. L. *Chemical Kinetics and Dynamics*; Prentice Hall: New York, 1989.  
 (64) McCosar, B. H.; Schanze, K. S. *Inorg. Chem.* **1996**, *35*, 6800.  
 (65) Ichino, T.; Fessenden, R. W. *J. Phys. Chem. A* **2007**, *111*, 2527.



The iodine radical anion,  $I_2^{\cdot-}$ , has been proposed to accept  $TiO_2(e^-)$ s and this data shows that the effective quantum yield for  $I_2^{\cdot-}$  formation is 1.20 for photons absorbed by tri-iodide.<sup>72</sup> Therefore, it is possible that power conversion efficiencies of operational solar cells are decreased more than what would be expected based simply on the competitive light absorption by tri-iodide. For mechanistic studies of dye sensitized solar cells, it should be emphasized that even with green light (532 nm), direct excitation of  $I_3^-$  occurs and the formation of radical intermediates needs to be accounted for in fundamental mechanistic experiments.

While the results here quite clearly implicate the sensitized formation of iodine atoms, it is not certain that they are involved in sensitizer regeneration in dye sensitized solar cells. Ruthenium bipyrazine compounds are potent photo-oxidants while sensitizers utilized in sensitized solar cells are strong photoreductants that oxidize iodide only after electron injection into  $TiO_2$ . The gold standard sensitizer in efficient dye sensitized solar cells is *cis*- $Ru(dcb)_2(NCS)_2$  ( $N3$ ) and its many derivatives, that is reported to have  $E^0(Ru^{III/II}) = 0.85$  V vs SCE.<sup>73</sup> Therefore, [*cis*- $Ru^{III}(dcb)_2(NCS)_2$ ] $^+$  ( $N3^+$ ) is a much weaker oxidant than the MLCT excited state of  $Ru(bpz)_2(deeb)^{2+}$ , by almost a full electronvolt.<sup>74</sup> Stanbury's recent estimate of the  $E^0(I^{\cdot-}) = 0.93$  V vs SCE implies that oxidation to the iodine atom by  $N3^+$  would be uphill by 70 mV.<sup>12</sup> We emphasize however, that iodide adsorption to  $TiO_2$  or Lewis acid–base interactions with the ambidentate thiocyanate ligand could activate iodide resulting in more favorable energetics for iodine atom formation. The possibility of iodine atoms as intermediates in sensitizer regeneration cannot be completely ruled out and their short lifetimes and optical properties would make spectroscopic detection difficult.

In photogalvanic solar cells, the excited state is quenched by hole transfer followed by thermal electron transfer into  $TiO_2$ .<sup>75–78</sup> It has previously been shown that the reduced ruthenium

compound studied here,  $Ru(bpz^{\cdot-})(bpz)(deeb)^+$  does not efficiently transfer electrons to  $TiO_2$  and that the yield can be improved by utilizing  $SnO_2$  which has a more favorable conduction band energy.<sup>28</sup> For application in photogalvanic cells or other energy conversion assemblies, the low cage escape yield (0.042) for excited state hole transfer will certainly be detrimental. Some of the factors that control cage escape yields have previously been elucidated for molecular excited states.<sup>79</sup> For organic sensitizers, electron transfer from singlet excited states generally yields low cage escape yields while triplet states yield redox products in quantitative yield.<sup>80,81</sup> The heavy Ru metal center effectively mixes the spin state through spin orbit coupling and cage escape yields that are intermediate between these extremes are generally reported.<sup>79</sup>

Outer-sphere adducts formed within the solvent cage may also influence the cage escape yield. Previous X-ray crystallographic studies have shown that iodide interacts with the carboxyl oxygens of the ethyl ester groups in the deeb ligand of  $Ru(bpy)_2(deeb)^{2+}$ .<sup>8</sup> In low dielectric constant solvents like  $CH_2Cl_2$ , evidence for ground state adducts with iodide were also observed.<sup>8</sup> If such interactions occur within the solvent cage, they could favor geminate back electron transfer. Indeed it was previously shown that the cage escape yield of  $I_2^{\cdot-}$  after hole transfer from  $Ru(bpy)_2(deeb)^{2+}$  increased by a factor of 2 when the ethyl ester groups were eliminated.<sup>8</sup> Therefore, there is good reason to believe that the quantum yields for cage escape and I–I bond formation can be improved through systematic variation of the excited state structure. In this regard, it is encouraging to note that Mallouk and co-workers found cage escape yields near unity after hole transfer from MLCT excited states to cyanometallate compounds.<sup>82</sup>

**Acknowledgment.** This work was funded by the Division of Chemical Sciences, Geosciences, and Biosciences, Office of Basic Energy Sciences of the U.S. Department of Energy through Grant DE-FC02-96ER14662. M.A. thanks the Swedish Research Council (Vetenskapsrådet) for a postdoctoral scholarship (623-2007-1038).

JA905021C

- (72) Bauer, C.; Boschloo, G.; Mukhtar, E.; Hagfeldt, A. *J. Phys. Chem. B* **2002**, *106*, 12693.  
(73) Yanagida, M.; Yamaguchi, T.; Kurashige, M.; Hara, K.; Katoh, R.; Sugihara, H.; Arakawa, H. *Inorg. Chem.* **2003**, *42*, 7921.  
(74) Nazeeruddin, M. K.; Kay, A.; Rodicio, I.; Humphry-Baker, R.; Mueller, E.; Liska, P.; Vlachopoulos, N.; Grätzel, M. *J. Am. Chem. Soc.* **1993**, *115*, 6382.  
(75) Albery, W. J. *Acc. Chem. Res.* **1982**, *15*, 142.  
(76) Ortman, I.; Moucheron, C.; Kirsch-De Mesmaeker, A. *Coord. Chem. Rev.* **1998**, *168*, 233.  
(77) Thompson, D. W.; Kelly, C. A.; Farzad, F.; Meyer, G. J. *Langmuir* **1999**, *15*, 650.  
(78) Nasr, C.; Hotchandani, S.; Kamat, P. V. *J. Phys. Chem. B* **1998**, *102*, 4944.

- (79) Hoffman, M. Z. *J. Phys. Chem.* **1988**, *92*, 3458.  
(80) Harriman, A.; Porter, G.; Wilowska, A. *J. Chem. Soc., Faraday Trans. II* **1983**, *79*, 807.  
(81) Holten, D.; Gouterman, M.; Parson, W. W.; Windsor, M. W.; Rockley, M. G. *Photochem. Photobiol.* **1976**, *23*, 415.  
(82) Mallouk, T. E.; Krueger, J. S.; Mayer, J. E.; Dymond, C. M. G. *Inorg. Chem.* **1989**, *28*, 3507.